

Supplementary Information for:

193 nm ultraviolet photodissociation for the characterization of singly charged proteoforms generated by MALDI

Kevin J. Zemaitis, Mowei Zhou, William Kew, and Ljiljana Paša-Tolić*

Environmental Molecular Sciences Laboratory, Pacific Northwest National Laboratory, Richland, Washington 99352, United States

Corresponding Author:

* Ljiljana Paša-Tolić – Email: ljiljana.pasatolic@pnl.gov

Contents:

Extended methods: sample preparation, MALDI-UVPD implementation, and operation.

Supplementary Figure S1: Digital photographs of the aligned excimer beam and UVPD optics chain on the instrument.

Supplementary Figure S2: Measured pulse energy and power of the 193 nm excimer beam after transmission through the optics.

Supplementary Figure S3: Zoomed insets of the non-annotated averaged spectrum of 3.0 mJ experiments and the full isolation spectrum of singly charged ubiquitin.

Supplementary Figure S4: Testing of HCD collision energy (CE) voltages for fragmentation of singly charged ubiquitin.

Supplementary Figure S5: Tracking of sequence coverage through additional averaging of 2 mJ, 3 mJ, and 4 mJ MALDI-UVPD experiments.

Supplementary Figure S6: Sequence coverage plots for 1 mJ, 2 mJ, 3 mJ, 4 mJ, and 5 mJ pulse energy experiments with the averaging of 100 microscans.

Supplementary Figure S7: Internal fragment sequence coverage maps from 1500 microscan experiments from clipsMS.

Supplementary Figure S8: Plot of photodepletion and sequence coverage for all experiments resultant from averaging of 1500 microscan events.

References.

Extended Methods: Sample Preparation, MALDI-UVPD Implementation and Operation:

CHEMICALS:

Ubiquitin from bovine erythrocytes, 2,5-dihydroxybenzoic acid (DHA), and trifluoroacetic acid (TFA, 99.5%) were from Sigma Aldrich (St. Louis, MO). Nanopure water and acetonitrile were HPLC grade and from Fisher Chemical (Fair Lawn, NJ).

DRIED DROPLET DEPOSITION:

Aqueous ubiquitin stock solution (1 mg/mL) was made and mixed in a 1:10 ratio (v/v) with DHA (15 mg/mL) dissolved within 90% acetonitrile with 0.1% TFA, 2.0 μ L droplets were spotted onto an indium-tin oxide (ITO) slide (Bruker Daltonics, Billerica, MA) for analyses.

SAFETY NOTE:

It is imperative to note that proper safety precautions should be followed in accordance with institutional environmental health and safety guidelines for the operation of a class of excimer laser used when not fully enclosed, the enclosure and optics should be evaluated for damage thresholds and proper protective equipment may include but is not limited to coverage of skin, proper rated laser safety goggles, laser safety curtains, and proper sign postage of the laboratory. Users should take care to follow all institutional environmental health and safety guidelines before application of UVPD.

MALDI-UVPD IMPLEMENTATION AND OPERATION:

Within our setup the excimer beam passes through two laser line mirrors (47-983, Edmunds Optics, Barrington, NJ) and the beam was cut prior to entering the HCD cell through a UV transmissible window mounted in a ConFlat flange with a set of irises (ID25SS and ID12Z, Thor Labs, Newton, NJ). The use of a stainless-steel iris to cut the beam, rather than the silver coated ceramic HCD exit lens, is highly desirable as to not accidentally damage the HCD cell when using high laser pulse energies for MALDI-UVPD. Mini pedestal extenders (SP-0.5E, Newport, Irvine, CA) are used to mount the irises within an Aegis Qube assembly (Newport, Irvine, CA), as shown within Supplementary Figure S1B. Mirrors were mounted within kinematic mounts (Q SS-100, Newport, Irvine, CA) in two separate Aegis Qubes and the beam was aligned with the C-trap removed to be concentric with the HCD exit and entrance lens as shown within Supplementary Figure S1C and S1D. If the excimer beam is not properly aligned inefficient UVPD and/or photoECD can occur,¹ and to aid in the ease of aligning the beam the beam path was shortened to the minimum distance with the laser positioned as close to the instrument as possible.

These Aegis Qubes also form a light tight enclosure; all panels and holes are covered with a combination of high-performance masking tape (T743-2.0, Thor Labs, Newton, NJ) and/or black aluminum foil which greatly reduces the risk of 193 nm excimer laser operation. When operating the laser, nitrogen flush gas flows through the excimer laser optics and into the light tight enclosure per the manufacturer's recommendation; this helps to also reduce the likelihood of surface damage from dust, etc. on the mirrored surfaces. Detailed measurements of laser power were obtained through the use of a S302C power meter and PM100D console (Thor Labs, Newton, NJ); measurements were made in triplicate at each pulse energy over an average of roughly 6 minutes, and these results are presented in Supplementary Figure S2. The laser beam had to be cut by the irises prior to measuring the pulse energy, and the irises were set to the diameter of the HCD exit lens to have accurate measurements of fluence within the HCD

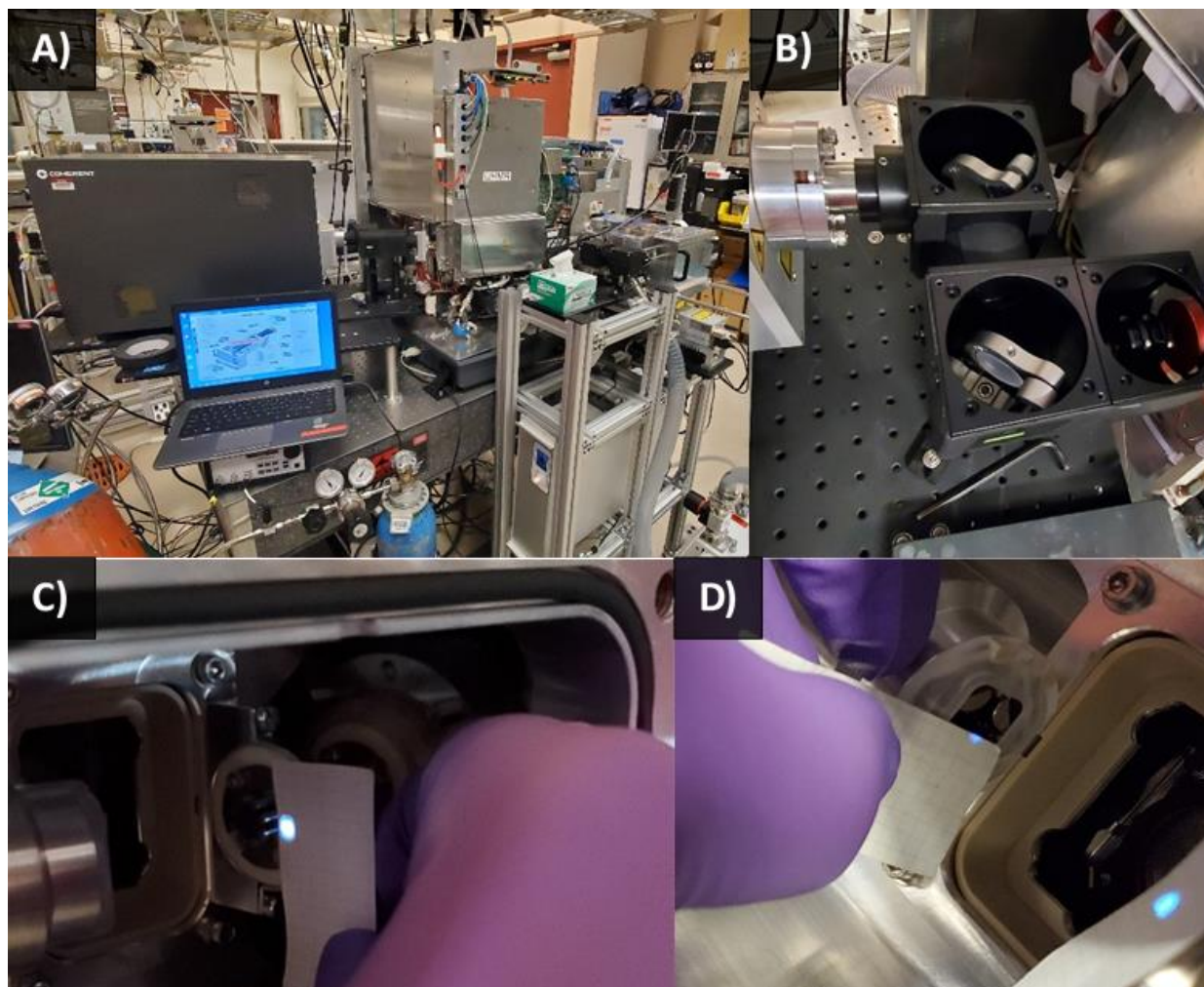
cell. Pulse energies were measured with the UV transmissible window in line and the attenuation of the excimer beam was found to be 73%.

For MALDI-UVPD experiments the excimer laser was operated in constant pulse energy mode, and for all experiments only one excimer laser pulse per dissociation event was used. All data acquired was saved as individual files resultant from spectral averaging and coaddition of various amounts of total transients (i.e., ~100, ~250, ~750, and a total of 1500). Coadditions of 5 “microscans” within the Tune window were utilized within MALDI-UVPD experiments. Each experiment which refers to a total microscan count corresponds to the total amount of spectral acquisitions (i.e., transients, analyzed pixels) coadded and averaged within the dataset. Data highlighting the benefits of additional averaging is shown in Supplementary Figure S4, and data solely for 100 averages is shown within Supplementary Figure S5.

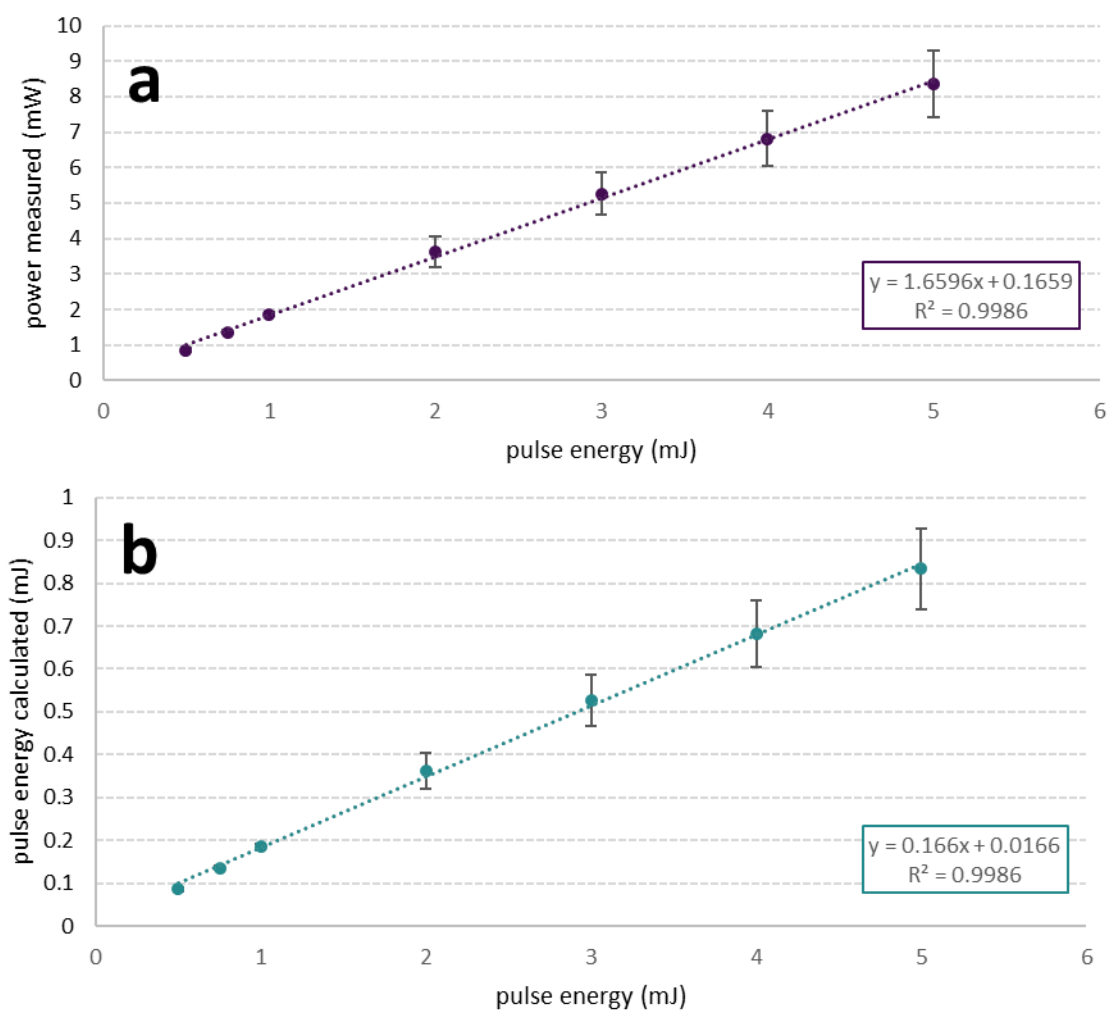
For all acquisitions the spectral noise thresholding was lowered to a setting of 2.0 (default is 4.54), full profile data was not acquired. Through the optimization of the instrumental parameters, it was found that the following parameters are critical to MALDI-UVPD experiments: detector m/z optimization was set to ‘low’ with RF amplitude of the injection flatapole, bent flatapole, and transfer multipole and HCD respectively tuned to 700 V, 940 V, and 1450 V for ubiquitin. The detection of low or high mass fragments is determined by the balance of these parameters and differs slightly from experiments with multiply charged species and for all MALDI-UVPD experiments as many of the large terminal fragments have $m/z > 5000$. The bent flatapole DC was 450 V and injection flatapole, inter-flatapole lens, and bent flatapole offset was 3.5 V, 2.5 V, and 1.5 V, respectively. All MALDI-UVPD experiments were completed with default timings used for HCD and can be compared to default settings for HCD with various CE voltages in Supplementary Figure S3.

The elevated pressure (EP)-MALDI source from Spectrograph, LLC and is equipped with a 2000 Hz Explorer One (349 nm) laser (Spectra Physics, Stahnsdorf, Germany).² The laser beam profile was measured at 30 μm diameter while the laser diode was set to 1.8 A to deliver a pulse energy of 6.48 to 6.6 μJ at 1000 Hz. The source was operated at a vacuum of 7 Torr, and the dual ion funnel source RF was initially autotuned and amplitude (V_{p-p}) adjusted with standards to optimize transmission, on the order of 150 and 250 V_{p-p} for the funnels, respectively. If not noted, default parameters provided by the manufacturer at installation were used. The fore vacuum of the MS was regulated at 0.98 mbar, and the ultra-high vacuum was measured at an average of 4.83×10^{-10} mbar with UHP argon trapping gas injected into the HCD cell and C-trap at a setting of 3.5 arbitrary units after recalibration of the flow controller. The MALDI source continually fires the laser during raster and a spatial resolution of 30 μm was set during these experiments. Ion accumulation was set to 500 ms for all experiments with a 512 ms transient acquisition (“240k” resolution at m/z 200) resulting in 500 laser shots per acquisition on dried droplets and an observed resolution of ~36k at m/z 8545. External calibration was performed using positive mode ESI direct infusion of 2 mg/mL solution of cesium iodide in isopropanol/water (50% v/v) at 5 $\mu\text{L}/\text{min}$.

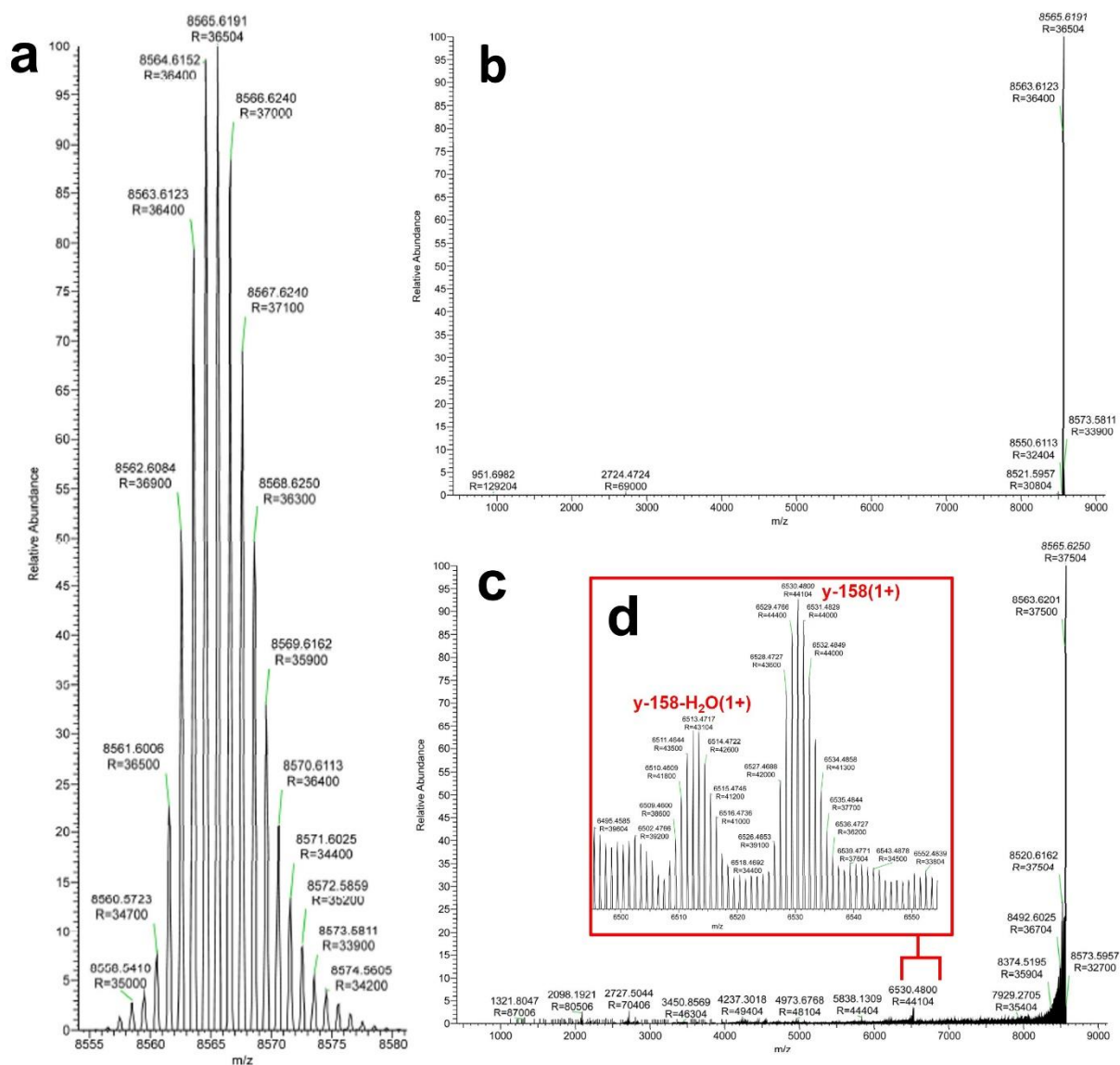
“IonGun” triggering of the UVPD experiment was used as described in greater depth within the original paper by Fort et al.³ Briefly, a pulse from the HCD axial field exit is sent and read by a Nano Every board (Arduino, Italy) flashed to monitor these additional pulses. The Arduino is programmed to send a trigger to a pulse/delay generator (Model 500, Berkeley Nucleonics Corp, San Rafael, CA), which generates a single TTL pulse input by BNC connection into the external triggering port of the ExciStar XS laser. The Arduino board is powered through USB connection and housed within a 3D printed case. Values of -150 V for the IonGun AxField Exit and a IonGun time of 5 ms were used within these experiments; varying the IonGun timing or the Arduino code can allow for multiple laser pulse experiments. Overall, the 20 V CE voltage used to initiate the “IonGun” triggering was found to not cause HCD fragmentation of the singly charged ubiquitin and HCD fragmentation was only seen at CE voltages > 200 V (data shown in Supplementary Figure S3).



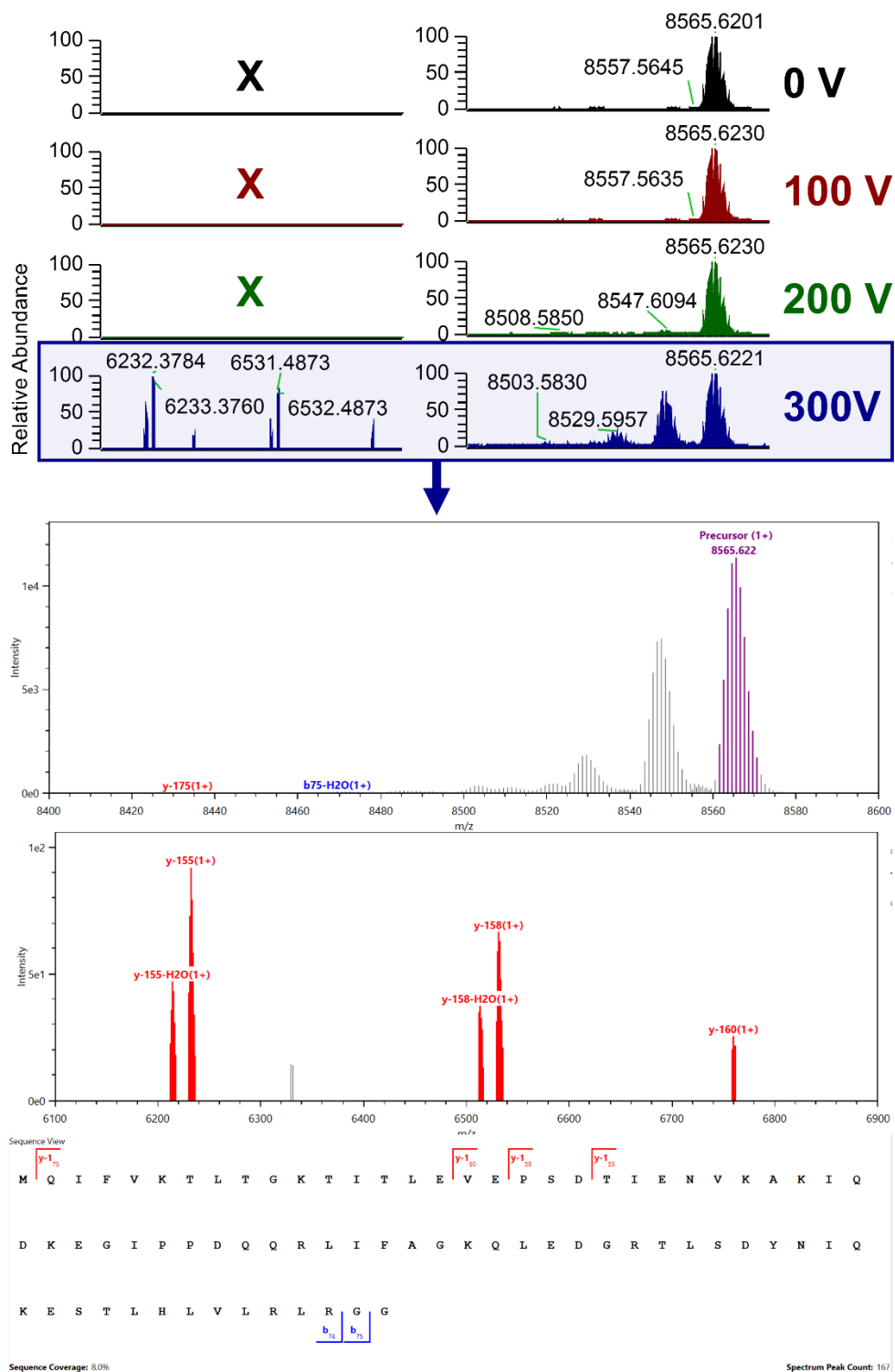
Supplementary Figure S1: (A) The instrument in its current configuration with the UHMR Q Exactive HF housed on a vibrationally isolated and dampened laser table with the Spectrograph EP-MALDI source attached and the UVPD excimer beam optics (B) fully enclosed in a light tight enclosure made from Aegis Qubes from Newport. The optics including mirror mounts, line mirrors, and the irises are shown in line within (B) where the power meter can be seen for measuring systematic transmission losses. Both (C) and (D) show alignment of the laser beam which is concentric with the entrance and exit lenses of the HCD trap; this was accomplished through removal of the C-trap. Reduction of the distance of the laser from the cell makes alignment of the beam an easier task and is highly advised.



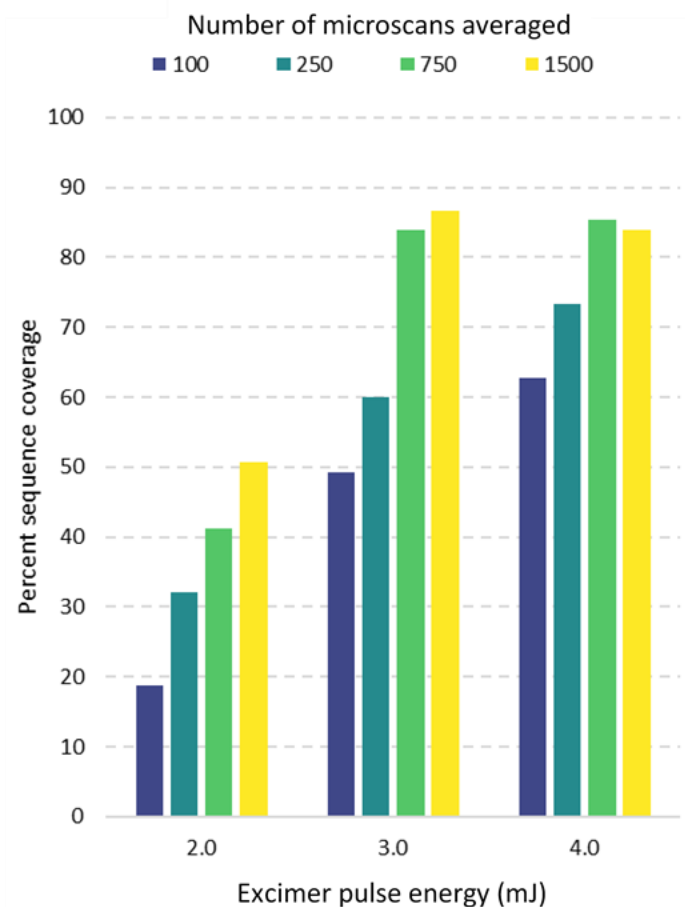
Supplemental Figure S2: (a) The measured power through the optics chain for set pulse energies and UV transmissible window by the Thor Labs PM100D console and SC301 power meter. The x-axis corresponds to the measured pulse energy from the Coherent Excistar XS from 0.5 mJ to 5 mJ output in constant energy mode. Transmitted pulse energy was calculated as shown in (b) with an observed attenuation of 73% for these experiments.



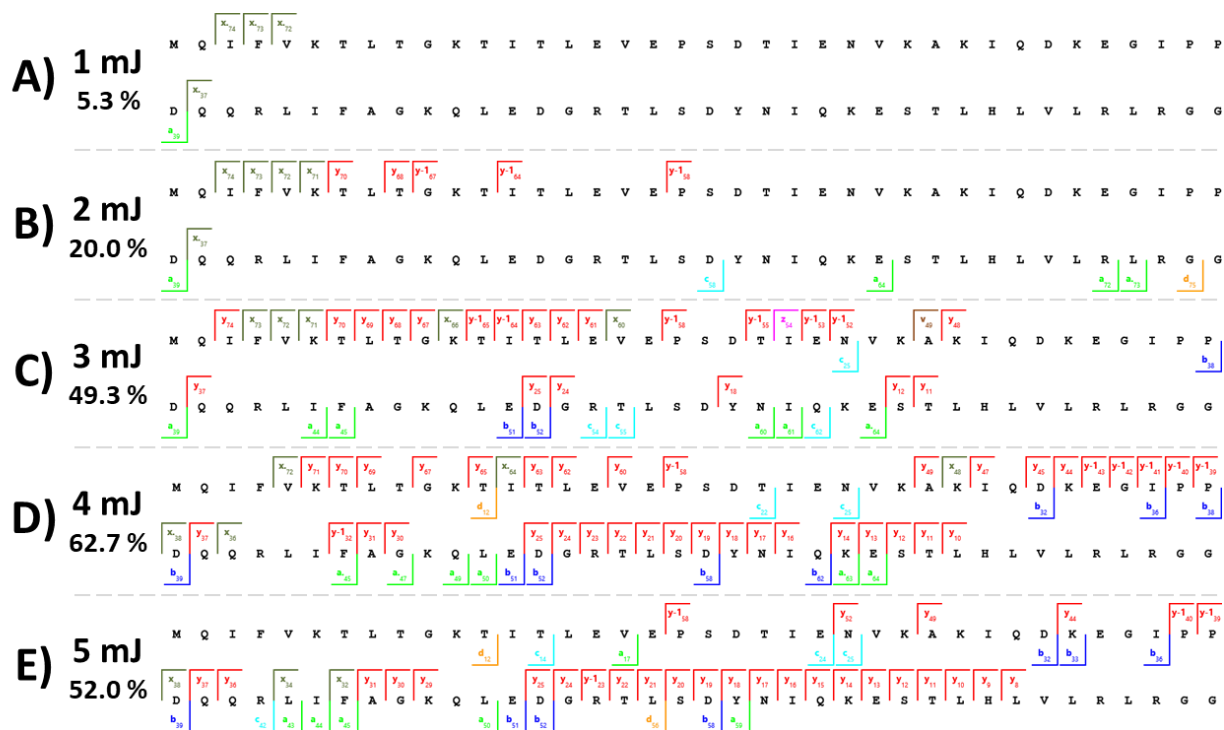
Supplementary Figure S3: (a) shows the isotopic distribution of baseline resolved ubiquitin within the MS1 isolation spectrum resultant from 1500 averages, which produced a signal-to-noise ratio (SNR) of 76,103 at m/z 8565; (b) is the full spectrum within the entire detected region of this MS1 isolation. (c) is the resultant spectrum from 3.0 mJ MALDI-UPVD experiments resultant from the averaging of 1500 microscans, where SNR at m/z 8565 was 18,023. Further, this spectrum highlights nearly complete isotopic distributions of fragment ions to roughly m/z 4000 (which can be further investigated in the raw spectrum provided in a supplementary .zip folder). (d) shows a zoomed region of interest from m/z 6480 to 6550 where the peak at m/z 6512 is the y -158- H_2O (1+) ion, and peak at m/z 6530 is the y -158 ion. These peaks correspond to a SNR of 319 and 558, respectively.



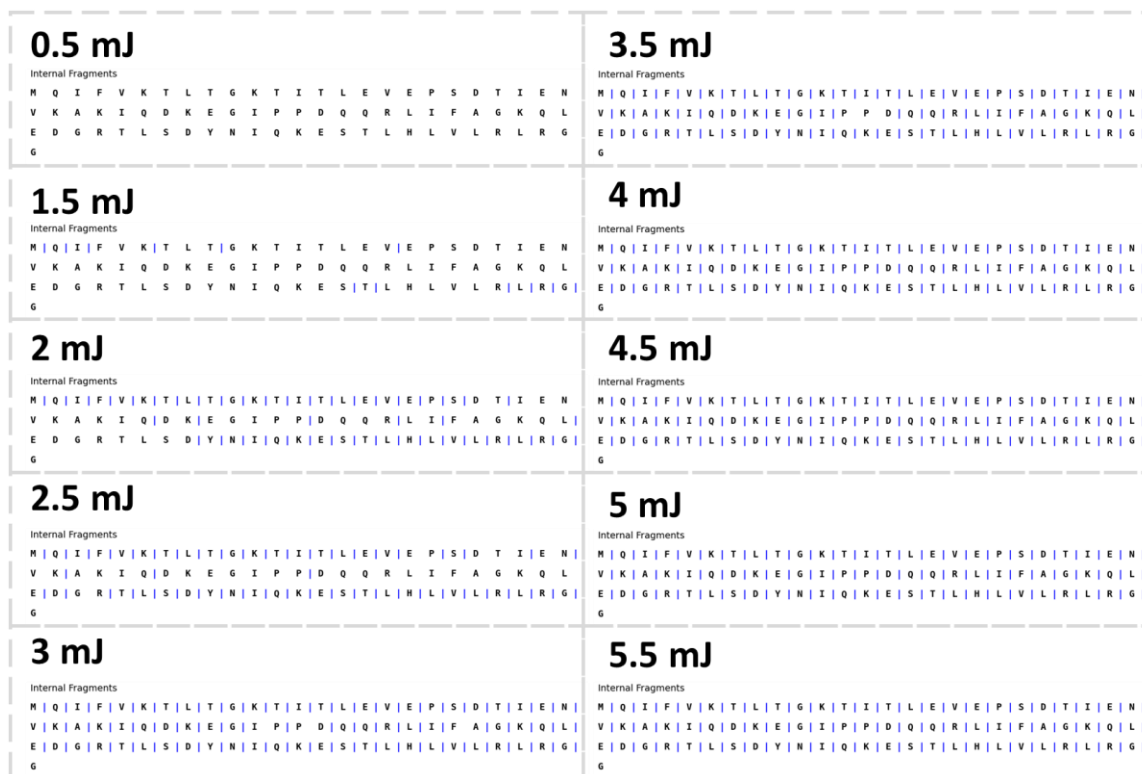
Supplementary Figure S4: HCD spectra with various CE voltages including 0 V, 100 V, 200 V, and 300 V. As demonstrated within the annotated spectrum from 300 V CE, fragmentation is observed with only several -b/-y type ions yielding only 8.0% sequence coverage of ubiquitin, and this was the highest achieved coverage with default HCD timings and voltages. While some water loss directly from the precursor is observed at 200 V, at the triggering voltage for IonGun experiments (20 V) no fragmentation can be observed although some levels of collisional activation are expected.



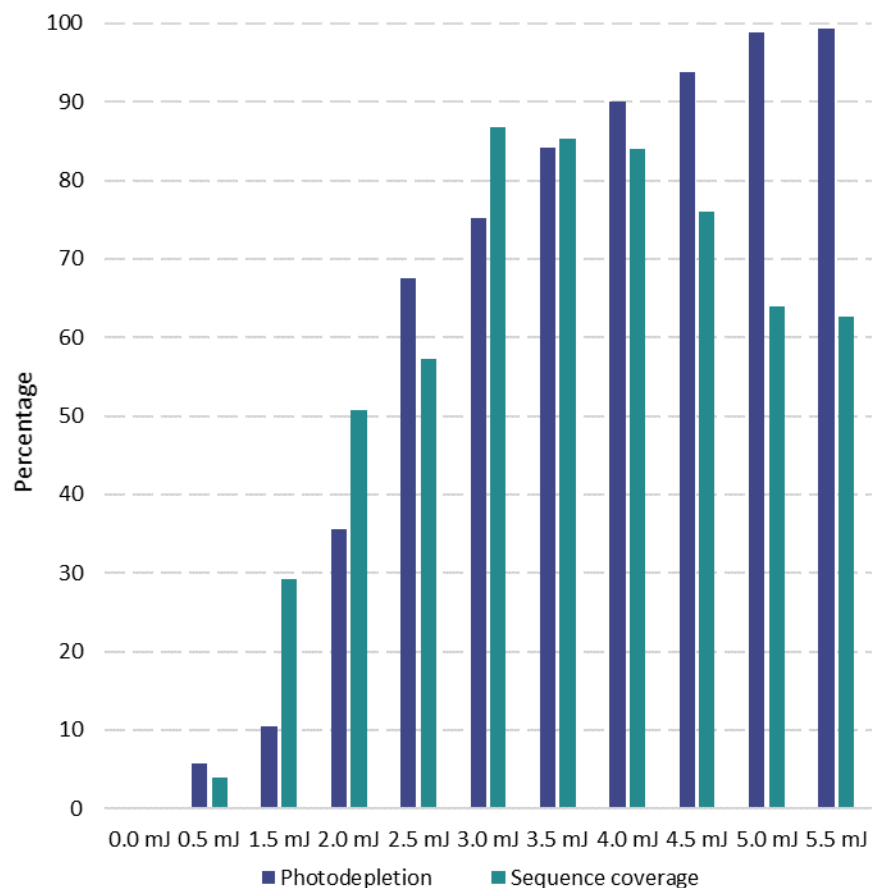
Supplementary Figure S5. Sequence coverage plotted as a function of microscan averaging for several pulse energies including 2 mJ, 3 mJ, and 4 mJ. The annotation was completed as stated within the main text, and spectra were annotated and visualized in LcMsSpectator (v1.1.7158.24217);⁴ all ion types (a, b, c, x, y, z) and side chain fragment ions (d, v, w) were annotated with possible neutral losses of water or ammonia with minimum SNR threshold of 1.5, Pearson correlation of 0.8, and relative intensity threshold of 3. Averages are from the same continuous acquisition and include averages of approximately 100, 250, 750 and 1500 microscans from each experiment. This demonstrates SNR boost through averaging with practical levels of sequence coverage for annotating proteins and proteoforms coming from low levels of only 100 microscans which took only 51.2 seconds versus high levels of sequence coverage from 1500 microscans which took 12.8 minutes. Further inclusion and annotation of internal fragments will significantly boost the sequence coverage per unit time.⁵ Currently, as presented within these experimental parameters 100 microscans corresponds to an analyzed area of the dried droplet corresponding to 0.09 mm² (100 acquisitions with an ablated area of 30 μm by 30 μm each).



Supplementary Figure S6: Sequence coverage maps from various MALDI-UVPD experiments including pulse energies of 1 mJ (A), 2 mJ (B), 3 mJ (C), 4 mJ (D), and 5 mJ (E) with the sequence coverage for each reported. While the maximum sequence coverage was obtained from conservative annotation of 1,500 microscans at 3 mJ pulse energy (Figure 1 in main text), varying the fluence of the laser cell can provide proportional gains at a lower number of averages. Where all data shown is for 100 averages, and this only includes conservative annotation of terminal fragments as previously described. This resulted in maximum sequence coverage of 62.7% with higher fluence at 4 mJ pulse energy, where comparable sequence coverage is annotated at 3.0 mJ pulse energy with 250 averages.



Supplementary Figure S7. Internal fragments as annotated through clipsMS.⁵ Spectra are from experiments with a total of 1500 averages and were processed with the Xtract algorithm within Freestyle. For input into clipsMS, all possible fragment ions under 20 amino acids in length were searched with constraints of 5 ppm error. It can be noted that within experiments employing greater than 1.5 mJ pulse energies increased rates of internal fragment ions are being produced, reaching a peak at 3.5 mJ pulse energies. Nearly complete sequence coverage can be noted from these experiments leading up to complete annotation of ubiquitin at 4 mJ solely from internal fragment ions. With further software development complete sequence coverage through terminal and internal fragments could be realized for many proteoforms.



Supplementary Figure S8. Photodepletion and sequence coverage are plotted as a function of microscans for several pulse energies including 2 mJ, 3 mJ, and 4 mJ. This includes the annotation of all ion types with neutral losses of water and ammonia from 1500 averages in each experiment. Photodepletion was calculated from the intensity value obtained from 1500 averages with triggering voltage, but no laser energy set. This shows that even within high fluence experiments there is enough precursor signal to include multiple laser shot experiments, but advanced manipulation of the ion packet may need to be tested and implemented for fragment ion protection (FIP),⁶ as to not induce over-fragmentation, especially of the large fragment ions which are predominant in these experiments.

References:

1. Shaw, J. B.; Robinson, E. W.; Paša-Tolić, L., Vacuum Ultraviolet Photodissociation and Fourier Transform–Ion Cyclotron Resonance (FT-ICR) Mass Spectrometry: Revisited. *Analytical Chemistry* **2016**, *88* (6), 3019-3023.
2. Belov, M. E.; Ellis, S. R.; Dilillo, M.; Paine, M. R. L.; Danielson, W. F.; Anderson, G. A.; de Graaf, E. L.; Eijkel, G. B.; Heeren, R. M. A.; McDonnell, L. A., Design and Performance of a Novel Interface for Combined Matrix-Assisted Laser Desorption Ionization at Elevated Pressure and Electrospray Ionization with Orbitrap Mass Spectrometry. *Analytical Chemistry* **2017**, *89* (14), 7493-7501.
3. Fort, K. L.; Dyachenko, A.; Potel, C. M.; Corradini, E.; Marino, F.; Barendregt, A.; Makarov, A. A.; Scheltema, R. A.; Heck, A. J. R., Implementation of Ultraviolet Photodissociation on a Benchtop Q Exactive Mass Spectrometer and Its Application to Phosphoproteomics. *Analytical Chemistry* **2016**, *88* (4), 2303-2310.
4. Park, J.; Piehowski, P. D.; Wilkins, C.; Zhou, M.; Mendoza, J.; Fujimoto, G. M.; Gibbons, B. C.; Shaw, J. B.; Shen, Y.; Shukla, A. K.; Moore, R. J.; Liu, T.; Petyuk, V. A.; Tolić, N.; Paša-Tolić, L.; Smith, R. D.; Payne, S. H.; Kim, S., Informed-Proteomics: open-source software package for top-down proteomics. *Nature Methods* **2017**, *14* (9), 909-914.
5. Lantz, C.; Zenaidee, M. A.; Wei, B.; Hemminger, Z.; Ogorzalek Loo, R. R.; Loo, J. A., ClipsMS: An Algorithm for Analyzing Internal Fragments Resulting from Top-Down Mass Spectrometry. *Journal of Proteome Research* **2021**, *20* (4), 1928-1935.
6. Holden, D. D.; Sanders, J. D.; Weisbrod, C. R.; Mullen, C.; Schwartz, J. C.; Brodbelt, J. S., Implementation of Fragment Ion Protection (FIP) during Ultraviolet Photodissociation (UVPD) Mass Spectrometry. *Analytical Chemistry* **2018**, *90* (14), 8583-8591.